Turkish Journal of Physics

Volume 33 | Number 1 Article 5

1-1-2009

Studies on Physical Properties and Carrier Conversion of SnO_2:Nd Thin Films

JOCHAN JOSEPH

VARGHESE MATHEW

JACOB MATHEW

K. E. ABRAHAM

Follow this and additional works at: https://journals.tubitak.gov.tr/physics

 Part of the Physics Commons

Recommended Citation

JOSEPH, JOCHAN; MATHEW, VARGHESE; MATHEW, JACOB; and ABRAHAM, K. E. (2009) "Studies on Physical Properties and Carrier Conversion of SnO_2:Nd Thin Films," *Turkish Journal of Physics*: Vol. 33: No. 1, Article 5. https://doi.org/10.3906/fiz-0707-4
Available at: https://journals.tubitak.gov.tr/physics/vol33/iss1/5

This Article is brought to you for free and open access by TÜBİTAK Academic Journals. It has been accepted for inclusion in Turkish Journal of Physics by an authorized editor of TÜBİTAK Academic Journals. For more information, please contact academic.publications@tubitak.gov.tr.

Turk J Phys
33 (2009) , 37 – 47.
© TÜBİTAK
doi:10.3906/fiz-0707-4

Studies on Physical Properties and Carrier Conversion of SnO_2:Nd Thin Films

Jochan JOSEPH[1], Varghese MATHEW[1], Jacob MATHEW[2], K. E. ABRAHAM[2]
[1] *St. Aloysius' College, Edathua, Kerala-INDIA*
[2] *Research Centre, S.B. College, Changanacherry, Kerala-INDIA*
e-mail: abrahamke@gmail.com

Received 10.07.2007

Abstract

Neodymium (Nd)-doped SnO_2 transparent conducting oxide thin films were prepared by vapour deposition technique under different deposition parameters: substrate temperature, time and flow rate of vapour deposition, amount of base material, distance between the substrate and spray gun tip, and dopant (Nd) concentration. The structural, optical, electrical and photo-electronic properties of the doped and undoped SnO_2 films were studied. X-ray diffraction studies shows the polycrystalline nature of the films with preferential orientation along the (101), (211) and (301) planes and an average grain size of 100 Å. The optical properties of these films were studied by measuring their optical transmission spectra in the UV-VIS-NIR range. Optical transmission is found to increase with Nd doping. Band gap, refractive index and thickness of the films were calculated. Its electrical properties were determined using four probe, Van der Pauw and Hall probe methods. On doping with Nd^{+3}, carrier conversion takes place from n-type to p-type; p-conductivity dominates. The resistivity of SnO_2 films changes from $91.9 \times 10^{-4}\Omega$m to $1.073 \times 10^{-4}\ \Omega$m as the substrate temperature varied 400–575 °C; and resistivity decreases initially on doping and increases as doping concentration increases. The minimum resistivity for the doped SnO_2 films was found to be $0.556 \times 10^{-4}\Omega$m at the deposition temperature 575 °C with 1 wt% concentration of the dopant. Photoconductivity and photovoltaic effects of doped SnO_2 films were also studied.

Key Words: Thin films, vapour deposition, x-ray diffraction, electrical properties, optical properties.

1. Introduction

Transparent conducting oxide thin films are of great interest due to its variety of applications. Consequently, thin films with high optical transparency and electrical conductivity have been a subject of investigation since last century [1–2]. Owing to its low resistivity and high transmittance, SnO_2 transparent conducting oxide

thin films are used as window layers and heat reflectors in solar cells [3–4], various gas sensors [5], LCDs etc. Now SnO_2 thin films have become an integral part of modern electronic technology. There are various methods such as spray pyrolysis, electron beam evapouration, chemical vapour deposition, magnetron sputtering and the Pechini method, etc., for the preparation of doped or undoped SnO_2 films [6]. The SnO_2 films are n-type semiconductors with a direct optical band gap of about 3.87–4.3 eV [7–8]. The valence band is closed shell of oxygen $2S^2$, $2P^6$ state mixed with some Sn states. The structure of the material in its bulk form is tetragonal rutile with lattice parameters $a = b = 4.737$ Å and $c = 3.816$ Å [9]. However in thin film form, depending on the deposition technique its structure can be polycrystalline or amorphous [10]. The grain size is typically 200–400 Å, which is highly dependant on deposition technique, temperature, doping level etc. [7–8]. SnO_2 films close to stoichiometric condition have low free carrier concentration and high resistivity, but non-stoichiometric SnO_2 films have high carrier concentration, conductivity and transparency. This comes about from an oxygen vacancy in the structure so that the formula for the thin film material is SnO_{2-x}, where x is the deviation from stoichiometry [7].

In_2O_3:Sn (ITO), SnO_2:F (FTO) and ZnO:Al (AZO) [11] are found to be conventional n-type, and $CuAlO_2$ and $SrCu_2O_2$ are found to be true p-type [12–14] transparent conducting oxide (TCO) thin films. N-type and p-type TCOs are useful in the fabrication of transparent p-n junctions as active elements in optoelectronic devices [15–16]. La doped n-type SnO_2 films with resistivity in the range of $1.064 \times 10^{-4}\Omega$m to $10.01 \times 10^{-4}\Omega$m and band gap in the range of 4.03–4.08 eV have been prepared recently by vapour deposition technique [17]. SnO_2 films are n-type direct-band gap semiconductors with high transparency and very good electrical conductivity, which find application in optoelectronic devices. P-type conducting transparent thin films of SnO2:Al [10] with resistivity in the range of $2.7 \times 10^{-4}\Omega$m to $90 \times 10^{-4}\Omega$m and band gap in the range of 4.105–3.604 eV, SnO2:Li [18] with resistivity in the range of $2.7 \times 10^{-4}\Omega$m to $1890 \times 10^{-4}\Omega$m and band gap in the range of 4.11–3.61 eV have been prepared by spray pyrolysis technique and Dy-doped SnO_2 films [17] with resistivity in the range $1.355 \times 10^{-4}\Omega$m to $9.85 \times 10^{-4}\Omega$m; and band gap in the range of 4.03–4.08 eV have been prepared recently by vapour deposition technique.

In this paper, similar to La and Dy-doped SnO_2 films, we are reporting the effect of Nd doping and the influence of deposition parameters on the structural, optical, electrical and photo electronic properties of SnO_2 films prepared by vapour deposition technique.

2. Experimental

The SnO_2 films were prepared by a vapour deposition technique with the help of a simple set up. We have chosen this technique because of the ease of selectivity of resistivity and transmittance by controlling deposition parameters. This technique is simple and cost effective due to fast deposition similar to spray pyrolysis. Moreover, the SnO_2 films produced possess large area and uniform coverage of the substrate. Experimental set up consists of a temperature-controlled hot plate (heater for the substrate), vapour spray gun and a 12 V DC driven air pump to control the flow rate. Dry air was used as carrier gas. Its flow rate was controlled by changing the current through the air pump. Optically plain glass substrate was cleaned with acetone and distilled water and was placed over the hot plate, heated to a particular temperature. AR grade $SnCl_2{\cdot}2H_2O$ from CDH was taken in the deposition unit and thermally evaporated. The $SnCl_2$ vapours formed

were deposited onto the heated glass substrate with the help of the air pump, which decomposes into Tin Oxide. The main reaction that leads to the formation of SnO_2 is [12]

$$SnCl_2(g) + O_2(g) \rightarrow SnO_2(s) + Cl_2(g) \uparrow . \tag{1}$$

The deposition parameters play an important role in the film formation. The films were prepared for different substrate temperatures from 400 to 600 °C. The time of vapour deposition was varied from 1 min to 5 min. The flow rate of vapour was varied by changing the speed of air pump from 1 arbitrary unit (AU) to 4 arbitrary units. Amount of $SnCl_2 \cdot 2H_2O$ taken in the deposition unit (3 g to 7 g) and the distance of the substrate from the vapour spray gun tip (1 mm to 5 mm) were also varied. The deposition parameters like substrate temperature, time of vapour deposition, flow rate, amount of $SnCl_2 \cdot 2H_2O$ and the substrate to spray gun tip distance were optimized for good conducting transparent SnO_2 films. All experiments for doping were performed at the optimized condition. Doped SnO_2 films were prepared by adding AR Grade $Nd(NO_3)_3 \cdot 6H_2O$ (CDH) at various concentrations from 1 wt% to 4 wt% in $SnCl_2 \cdot 2H_2O$.

3. Results and Discussion

3.1. Structural Properties

Structure of the doped and undoped SnO_2 films were studied by taking XRD using Cu Kα (λ = 0.154056 nm) radiation from Bruker, D8 Advance, Germany and were compared with JCPDS data card. The XRD patterns of SnO_2 films prepared at various substrate temperatures are shown in Figure 1. The film coated at 575 °C is found to be better and shows a polycrystalline nature oriented along the (101), (211) and (301) planes at $2\theta = 34.281°$, $52.156°$ and $66.285°$, respectively with single phase SnO_2. Figure 2 shows the XRD patterns with d and (hkl) values of SnO_2 films prepared at 575 °C substrate temperatures. The XRD patterns are consistent with those reported in [6, 10]. The presence of other orientations such as (110), (200), (220), (310) was also detected with lower intensities. The low intensity of the appeared planes indicates low crystallinity and tiny crystallite size. Figure 3 shows a photograph (×40) of SnO_2 thin film taken with an Olympus CX-31 Trinocular Microscope. On Nd doping at 575 °C, the XRD shows no peaks corresponding to Nd or its compounds, but the intensity of SnO_2 peaks decreased. The decrease in peak intensities is basically due to the replacement of Sn^{4+} ions with Nd^{3+} ions in the lattice of SnO_2 film, as was done in [19–20]. This process leads to the shifting of Sn^{4+} ions to the interstitial sites and also an increase in the amorphous phase. The XRD pattern of SnO_2 films doped at different concentrations of Nd is given in Figure. 4. The average grain size was calculated by using Scherrer formula [19]

$$D = K\lambda/\delta\omega \cos\theta, \tag{2}$$

where D is the average crystalline size, K is a constant (~ 1), λ is the wavelength, $\delta\omega$ is the FWHM of peaks and θ is the Bragg angle. The increase in temperature enhances the preferred orientation with an increase in grain size. The increase in substrate temperature may cause decrease of the density of nucleation centres and, under these circumstances, a smaller number of centres start to grow, which results in large grains [17].

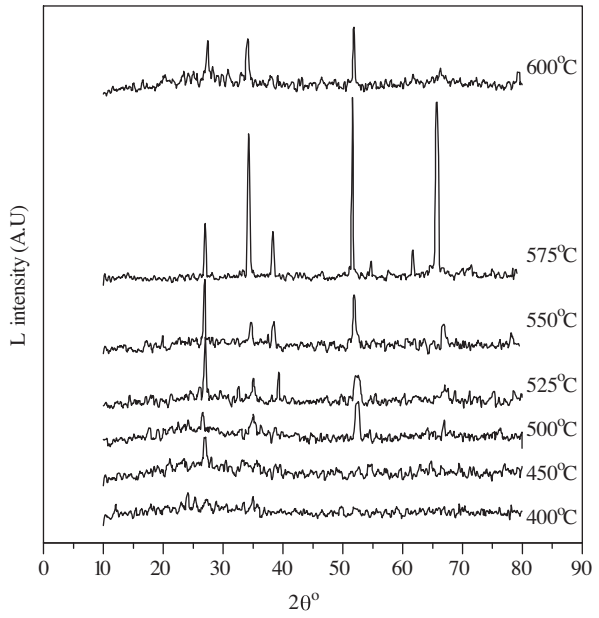

Figure. 1 X-ray Diffraction pattern for SnO_2 films at different substrate temperature.

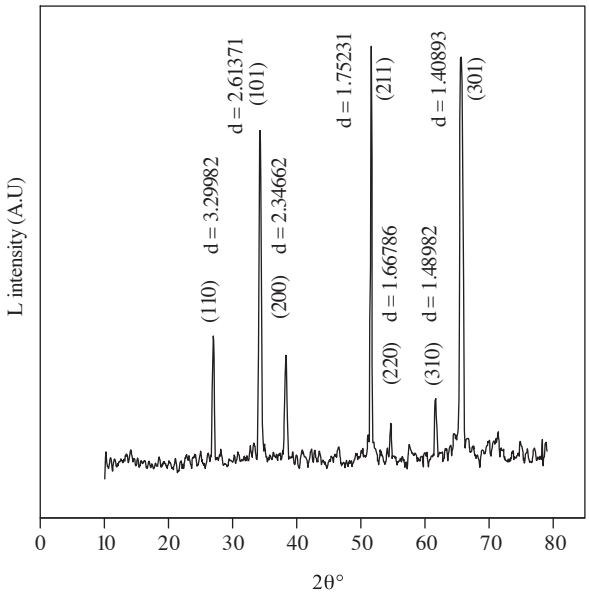

Figure. 2 X-ray Diffraction pattern for SnO_2 films with d & (hkl) values at 575 °C.

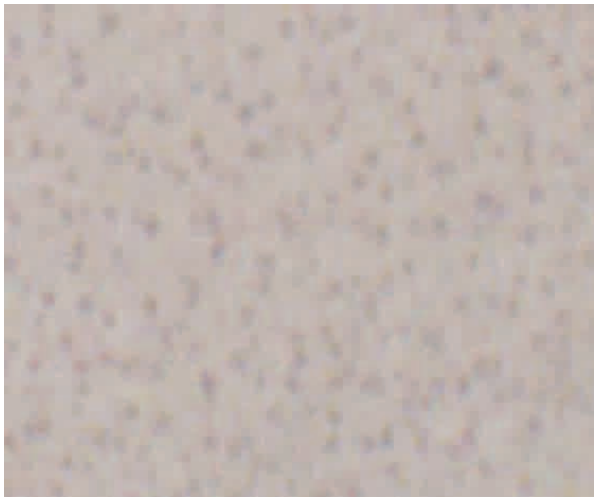

Figure 3. Photograph of SnO_2 thin film.

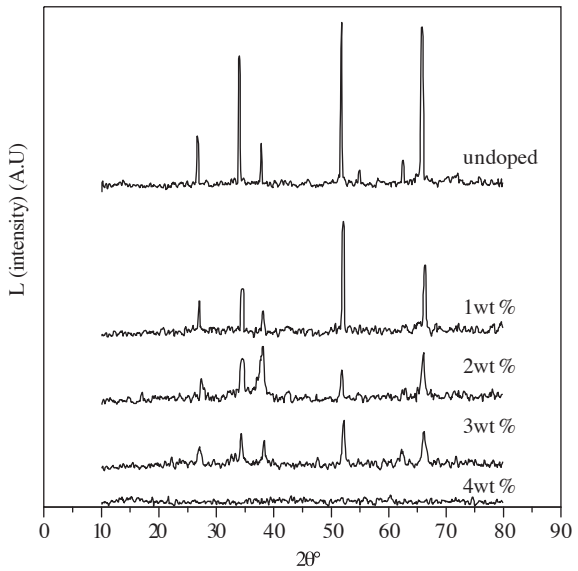

Figure 4. X-ray Diffraction pattern for Nd-doped SnO_2 films for different concentrations of dopant.

3.2. Optical Properties

The UV-VIS-NIR transmittance spectra of the SnO_2 films prepared at various temperatures and at different concentrations of Nd were recorded via a Varian Cary 5000 UV-VIS-NIR spectrometer, and are shown in Figures 5–7. As temperature increases, optical transmission T (%) increases. This may be due to the decrease in thickness t and increase in film homogeneity and crystallinity revealed in the XRD.

Films prepared at deposition temperature 575 °C with 1 wt% and 2 wt% of Nd exhibit a transmission of >75% in the visible region. The transmittance of the films was also influenced by a number of minor effects, which include surface roughness and optical inhomogeneity in the direction normal to the film surface. Absorption coefficient α, optical band gap E_g, refractive index μ and thickness t of the films were evaluated from the transmittance/absorption spectra. The evaluation of absorption coefficient α was using the equation [20–21]

$$\alpha = 2.303A/t, \tag{3}$$

where t is the thickness and A is the absorbance of the SnO_2 films. The direct optical band gap E_g was determined by fitting the absorption data to the equation [22]

$$\alpha h\nu = B(h\nu - E_g)^{1/2} \tag{4}$$

It is found that E_g increases with substrate temperature (Figure 8). It also increases at low concentrations but decreases at higher concentrations (Figure 9). The refractive index and thickness (t) of the film were determined by Swanepoel technique [23]. The refractive index of the film is found to be ∼1.8 and thickness is ∼1.5 μm (at 575 °C). The value of refractive index seems to be in good agreement with earlier results [6].

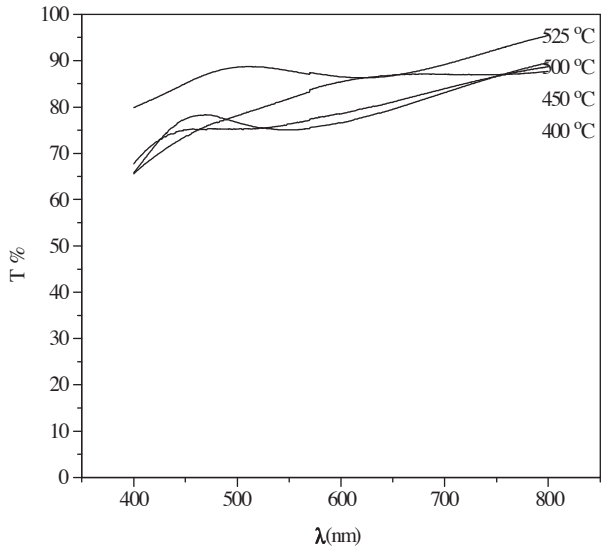

Figure 5. Optical Transmittance T (%) versus wavelength λ of SnO_2 films at substrate temperature 400–525 °C.

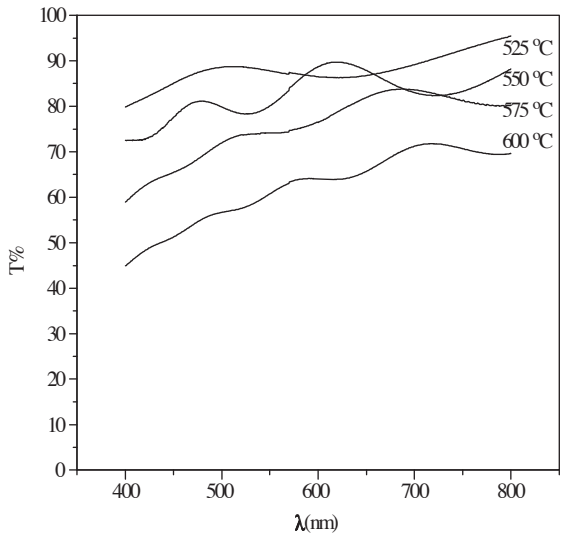

Figure 6. Optical Transmittance T (%) versus wavelength λ of SnO_2 films at substrate temperature 525–600 °C.

3.3. Electrical Properties

Electrical parameters of the SnO_2 films were measured by four probe, Van der Pauw and Hall probe methods. 1 cm × 1 cm size samples were cut from large samples for electrical measurements. In order to determine the mobility and sheet resistance, a combination of a resistivity measurement and Hall measurement is needed. The objective of Hall measurement in the Van der Pauw technique is to determine the carrier concentration from the Hall voltage. Table 1 gives the results of four probe, Van der Pauw and Hall probe

measurements for undoped films at different substrate temperature and Table 2 gives that of SnO_2 films at different concentration of Nd.

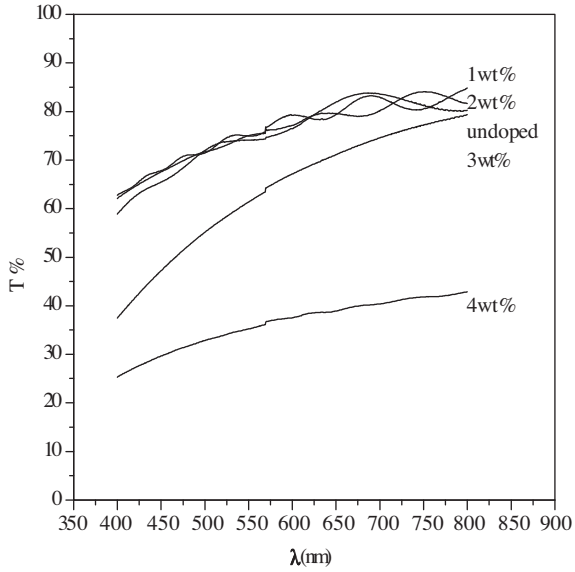

Figure 7. Optical Transmittance T (%) versus wavelength λ of Nd-doped SnO_2 films at different concentrations of dopant.

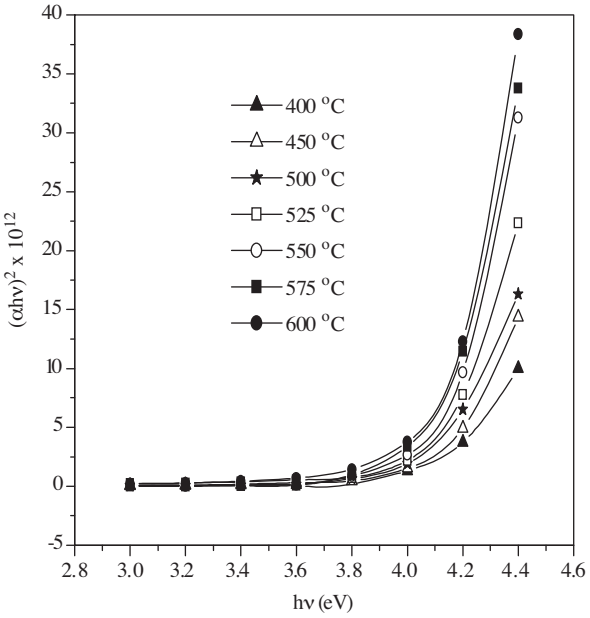

Figure 8. $(\alpha h\nu)^2$ versus $h\nu$ graph of SnO_2 films at different substrate temperature.

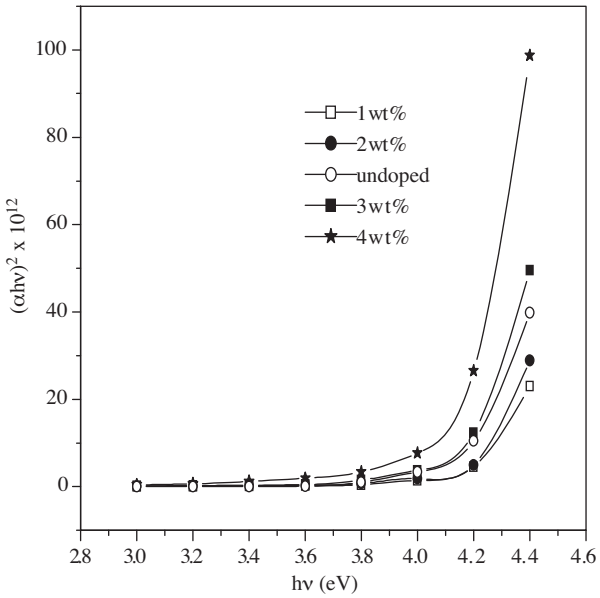

Figure 9. $(\alpha h\nu)^2$ versus $h\nu$ graph of Nd doped SnO_2 films at different concentrations of the Dopant.

By measuring the sheet resistance using the equation

$$R_s = (\pi/\ln 2)(R_{ab,cd} + R_{bc,da})/2 \tag{5}$$

and the average thickness t of the film, its resistivity was calculated from equation

$$\rho = R_s \cdot t \tag{6}$$

where $R_{ab,cd}$ is measured by forcing a current from contacts (at corners) a to b, then measuring the voltage between the contacts d and c. These values of ρ are in good agreement with that obtained from Four Probe method. R_s and ρ of Nd doped SnO_2 films is found to be lower than undoped SnO_2 films. To measure the Hall voltage V_H a current I is forced through contacts a and c and the

Table 1. Electrical parameters of undoped SnO_2 films.

Concentration of Nd (wt%)	R_s ($\Omega/\square$)	$\rho_{fourprobe}$ ($10^{-4}\Omega$m)	$\rho_{vanderpauw}$ ($10^{-4}\Omega$m)	B (T)	I (mA)	V_H (mV)	μ_H (m^2/v/s)	n (p) (N/m^3)
400	161K	112	91.9	0.2	1	-56.1	0.0174	3.89×10^{22}
450	4.8K	28.6	29.02	0.2	1	-31.4	0.0327	6.57×10^{22}
500	920	7.96	8.02	0.2	1	-12.2	0.0663	1.17×10^{23}
525	166.56	1.865	1.935	0.2	1	-2.8	0.081	3.98×10^{23}
550	78.29	1.21	1.093	0.2	1	-1.3	0.083	6.88×10^{23}
575	71.27	1.16	1.073	0.2	1	-1.2	0.0842	6.91×10^{23}
600	585.4	12.6	10.25	0.2	1	-5	0.0427	1.42×10^{23}

Hall voltage V_H is measured across the remaining pair of contacts b and d by applying a constant magnetic field B perpendicular to the plane of the sample film. The effect of background (drift) voltage in the absence of magnetic field was taken into account and compensated. The charge carrier concentration n (p) and Hall mobility μ_H can be determined from the following equations:

Table 2. Electrical parameters of Nd doped SnO_2 films.

Concentration of Nd (wt%)	R_s ($\Omega/\square$)	$\rho_{fourprobe}$ ($10^{-4}\Omega$m)	$\rho_{vanderpauw}$ ($10^{-4}\Omega$m)	B (T)	I (mA)	V_H (mV)	μ_H (m^2/v/s)	n (p) (N/m^3)
0	71.27	1.16	1.073	0.2	1	-1.2	0.0842	6.91×10^{23}
1	37.05	0.62	0.556	0.2	4	+0.1	0.00337	3.33×10^{25}
2	49.85	0.81	0.748	0.2	3	+0.1	0.00334	2.49×10^{25}
3	62.54	1.1	0.938	0.2	2	+0.1	0.0039	1.66×10^{25}
4	121.9	2.3	1.82	0.2	3	+0.2	0.0027	1.25×10^{25}

$$n(p) = IB/(q|V_H|t) \tag{7}$$

$$\mu_H = |V_H|/(R_s \cdot IB). \tag{8}$$

The sign of the Hall voltage determines the type of the carriers (+ for p-type, - for n-type). Sn forms an interstitial bond with oxygen and exists either as SnO or SnO_2; hence has a valency of +2 or +4, respectively. This valency state has a direct bearing on the ultimate conductivity of Tin Oxide. The lower valence state results in a net reduction in carrier concentration since a hole is created which acts as a trap and reduces conductivity. On the other hand, predominance of SnO_2 state means Sn^{4+} acts as an n-type donor-releasing electron to the conduction band. The large value of n indicates that Sn forms bond with oxygen and exists as

SnO_2. It is found that the undoped SnO_2 films behave as n-type semi-conductors. On Nd doping, majority carriers convert from electrons to holes and become p-type semi-conductor. Here, Nd^{+3} acts as acceptors in the Sn^{4+} sites and hence p-conductivity increases. On doping (1 wt% of Nd) carrier concentration increases from 6.91×10^{23} N/m^3 to 3.33×10^{25} N/m^3 with a reduction in R_s from 71.27 $\Omega/$ to 37.05 $\Omega/$ and ρ from 1.073 $\times 10^{-4}\Omega$m to 556 $\times 10^{-4}\Omega$m. The decrease in resistivity with temperature may be attributed to the growth of grain size and improvement of film homogeneity. The variations of resistance of SnO_2 films with respect to the deposition parameters are given in Figures 10–14. These figures reveal the optimum deposition parameters for highly conducting transparent films.

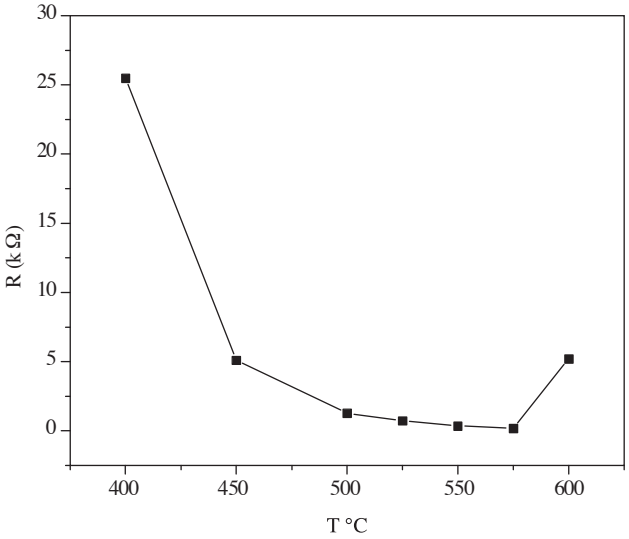

Figure 10. Variation of resistance of SnO_2 films with substrate temperature.

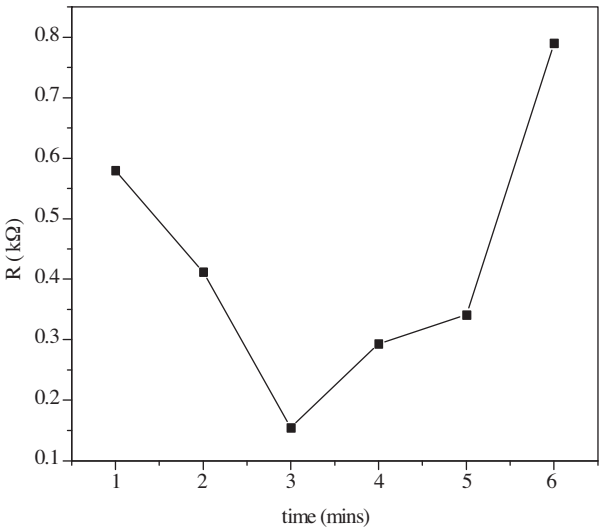

Figure 11. Variation of resistance of SnO_2 films with time of vapour deposition.

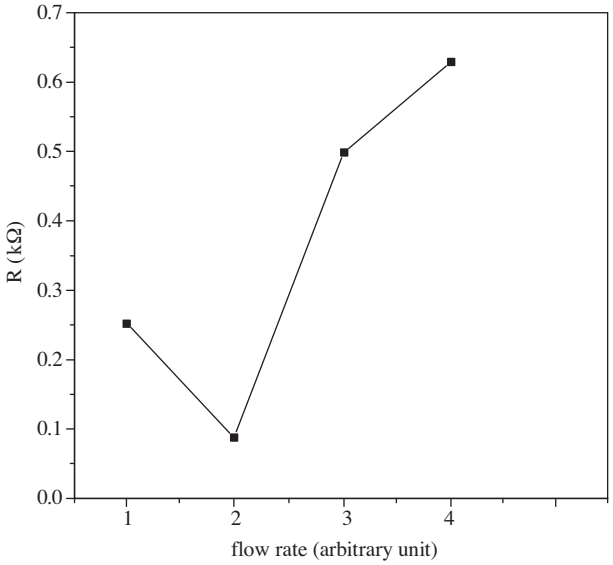

Figure 12. Variation of resistance of SnO_2 films with flow rate of vapour deposition.

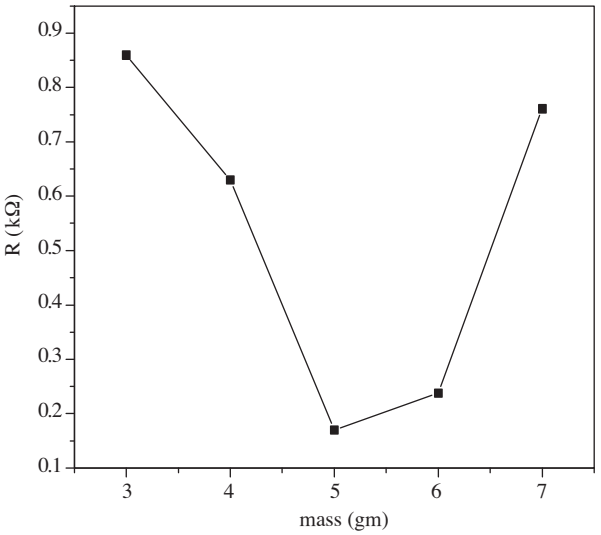

Figure 13. Variation of resistance of SnO_2 films with mass of base material.

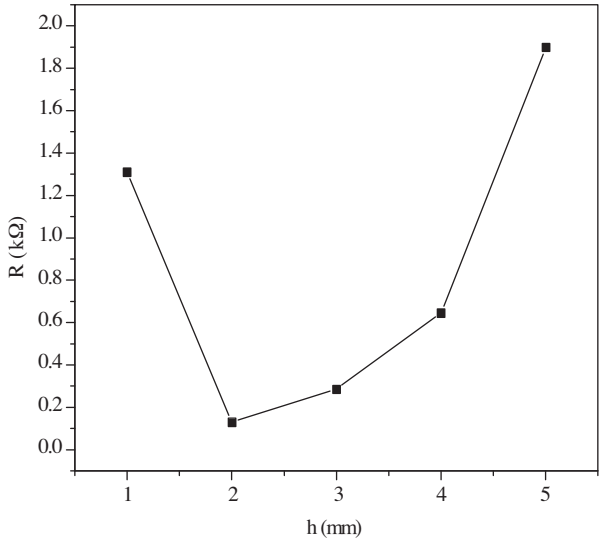

Figure 14. Variation of resistance of SnO_2 films with distance of the substrate from vapour source.

3.4. Photoconductivity and photovoltaic properties

PC and PV studies of Nd doped SnO_2 films were performed by using a 100 W milky lamp as excitation source. Figure 15 and Figure 16 shows variation of photocurrent (PC) and photo voltage (PV) of SnO_2 films with concentration of Nd. It is observed that the maximum photocurrent occurs at 2 wt% and maximum photo voltage occurs at 1 wt% of Nd. Table 2 shows maximum carrier concentration at 1 wt% doping. Hence maximum PV occurs at 1 wt% of Nd, which may be due to maximum number of charge separation. In the case of PC, the largest carrier concentration at 1wt% of Nd causes more carrier collision probability during charge transport which in turn reduces the photoconductivity. At 2 wt% of Nd the charge concentration seems to be optimum for better PC. But higher percentage of Nd reduces charge concentration and hence PC and PV.

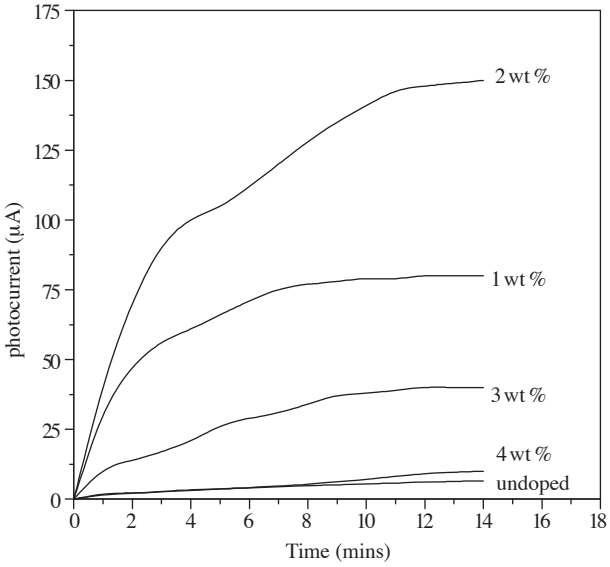

Figure 15. The rise of Photocurrent of Nd doped SnO_2 films with time for different concentrations of the dopant.

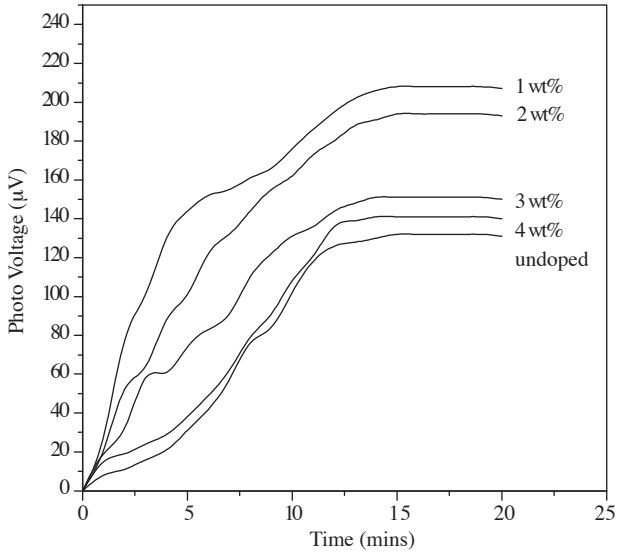

Figure 16. The rise of Photo voltage of Nd doped SnO_2 films with time for different concentrations of the dopant.

4. Conclusion

The structural property, electrical conductivity and optical transmittance of SnO_2 films depend highly on the deposition parameters. XRD analysis shows that the films coated are SnO_2. Undoped SnO_2 films are found to be n-type semiconductors and at 575 °C deposition temperature. It gives high conductivity ($\rho = 1.073 \times 10^{-4}\Omega$m) and good optical transmission $> 70\%$ with sheet resistance 71.27 $\Omega/$ and $E_g = 4.08$ eV. The refractive index of the film is $\sim$1.8. The thickness of the SnO_2 films were found by Swanepoel envelope technique and obtained as 1.5 μm at 575 °C. The absorption coefficient is of the order of 10^5 /m. The doping effect of Nd in the structural, photo electronic, electrical and optical properties of SnO_2 films were investigated. XRD pattern of Nd doped SnO_2 films shows a decrease in the intensity at all the planes which is due to the replacement of Sn^{4+} ions with the Nd^{3+} ions and also due to the increase in the amorphous background. Optical transmission is found to be increased on Nd doping. PC and PV effects of SnO_2 films increase on Nd doping. E_g of doped SnO_2 films is found to vary from 4.06–4.11 eV. On doping, carrier conversion takes place from n-type to p-type and conductivity enhances remarkably. The increase in conductivity is due to the increase in carrier concentration. The best film giving relatively good transparency ($> 75\%$) and conductivity ($\rho = 5.56 \times 10^{-5}\Omega$m) is found to be that doped at 1 wt% of Nd.

Acknowledgements

One of the authors, Mr. Jochan Joseph acknowledges the University Grants Commission, India for providing FIP Scheme under X plan.

References

[1] M. Penza, S. Cozzi, M. A. Tagliente, L. Mirenghi, C. Martucci and A. Quirini, *Thin Solid Films.*, **71**, (1999), 349.

[2] S. Ishibashi, Y. Higuchi, Y. Ota and K. Nakamura, *J. Vac. Sci. Technol.*, **A8**, (1998), 1403.

[3] G. Frank, E. Kaur and H. Kostlin, *Solar energy Matter.*, **8,** (1983), 387.

[4] S. Colen, *Thin Solid Films.*, **77**, (1981), 127.

[5] K. Nomura, Y. Ujihira and S. S. Sharma, *J. Mater. Sci.*, **24**, (1989), 937.

[6] K. S. Shamala, L. C. S Murthy, and K. Narasimha Rao, *Bull. Mater. Sci.*, **27**, (2001), 295.

[7] K. L. Chopra, S. Major, and D. K. Pandya, *Thin Solid Films.*, **102**, (1983), 1.

[8] T. J. Coutts, D. L. Young, and X. Li, *MRS. Bull.*, **25**, (2000), 58.

[9] A. L. Dawar and J. C. Joshi, *J. Mater. Sci.*, **19**, (1984), 1.

[10] M. M. Bagheri-Mohagheri and M. Shokooh-Saremi, *J. Phys. D: Appl. Phys.*, **37,** (2004), 1248.

[11] A. J. Freeman, K. R. Poeppelmeirer, T. O. Mason, R. P. H. Chang, and T. J. Marks, *MRS Bull.*, **25**, (2000), 45.

[12] H. Yanagi, H. Kawazoe, A. Kudo, M. Yasukowa, and H. Honoso, *J. Electro ceram.*, **4**, (2000), 427.

[13] A. Kudo, H. Yanagi, H. Hosono, and H. Kawasoe, *Appl. Phys. Lett.*, **73**, (1998), 220.

[14] H. Kawazoe, H. Yanagi, K. Ueda and H. Hosono, *MRS Bull.*, **25**, (2000), 28.

[15] J. Tate, M. K. Jayaraj, A. D. Draeseke, T. Ulbrich, A .W. Sleight, K. A. Vanaja, R. Nagarajan, J. F Wager and R. L Hoffman. *Thin Solid Films.*, **397**, (2002), 119-24.

[16] M. K. Jayaraj, A. D. Draeseke, J. Tate, A. W. Sleight, N. Duan, *Mater. Res. Soc. Symp. Proc.*, **666**, (2001).

[17] J. Joseph, V. Mathew and K. E. Abraham, *Cryst.Res.Technol.*, **41**, (2006), 1020.

[18] M. M. Bagheri-Mohagheri and M. Shokooh-Saremi, *Semi cond. Sci. Tecnol.*, **19**, (2004), 764.

[19] X. C. Yang, *Mater. Sci. Eng.*, **B 93**, (2002), 249.

[20] A. D. Yoffe, *Adv. Phys.*, **42**, (1993), 173.

[21] W. T. Dong, X. S. Wu, D. P. Chen, X. W. Jiang, and C. S. Zhu, *J. Chem. Lett.*, **5**, (2004), 496.

[22] J. I. Pankove. *Optical Processes in Semiconductors*, N. Holonyak (Eds.) Solid State Physical Electronics Series, (Prentice Hall, Eagle Wood Cliffs, N. J., USA, 1971).

[23] R. Swanepoel, *J. Phys. E.*, **16**, (1983), 121.